Materials Science-Poland
Volume 43 Issue 1 · pp. 42–50 · DOI: 10.2478/msp-2025-0004

Materials Science-Poland

Bonding mechanism between the AlN ceramic matrix and the copper-based metal cladding layer

Research Article

Song Wang[1], Hao Lu[2], Fengyuan Shu[3], Xin Zhang[4]*, Guibian Li[5]

[1] *State Power Investment Group Yunnan International Power Investment Co., Ltd, Kunming, 650228, China*
[2] *School of Electrical Engineering, Xinjiang University, Urumqi, 830046, China*
[3] *School of Chemical Engineering and Technology, Sun Yat sen University, Zhuhai, 519082, China*
[4] *New Energy Technology Research Institute, State Power Investment Corporation Science and Technology Research Institute, Beijing, 102218, China*
[5] *Shanxi Fenglei Drilling Tools Co. Ltd., Houma, 043001, China*

Received 06 May 2024; Accepted 09 February 2025

Abstract: High-temperature brazing and laser cladding methods can form a good metallurgical bond between ceramics and copper cladding. Herein, through these two methods, the preparation of a Cu-based metal cladding layer on the surface of aluminum nitride (AlN) ceramics was carried out. Scanning electron microscopy, X-ray diffraction, energy-dispersive spectroscopy, and other characterization techniques were employed to observe the macroscopic and microscopic morphologies, elemental distribution, and microstructure characteristics of Cu-based metal coatings and transition layers, in order to analyze the interface bonding mechanism. Research has found that the active element titanium (Ti) has a significant promoting effect on the wettability of Cu powder on the surface of ceramics. Metallurgical reactions occur at the interface between ceramics and Cu-based metal coatings. Al and N elements in ceramics react with most of the Ti in the metal coating and Cu in the molten metal also reacts with Ti, generating new compounds, thereby forming a metallurgical bond between ceramics and Cu coatings.

Keywords: *Laser cladding • Ceramic substrate • Elemental distribution • Microstructure*

1. Introduction

With the rapid development of the electronic industry, electronic components are developing toward high integration and high power. This tendency makes a high demand on the performance of packaging materials and packaging technology. Therefore, the performance of the substrate material, such as high thermal conductivity, thermal expansion coefficient matched with the chip material, and excellent electrical and mechanical properties, is in high demand. Presently, the ceramic materials with good performance include aluminum nitride (AlN) ceramics, Al_2O_3 ceramics, BeO ceramics, boron nitride (BN) ceramics, diamond ceramics, and cubic BN ceramics [1]. However, the properties of some ceramics greatly limit application in the production of electronic components [2]. In comparison, AlN ceramics have advantages in price and metallization [3].

Physical vapor deposition (PVD) techniques are widely employed to deposit various materials onto different substrates. These techniques are generally classified by the methods used to evaporate the target material for deposition. PVD methods are popular in industrial applications due to the hard and durable coatings they produce, which can be applied to both organic and inorganic substrates. However, the high temperature and high vacuum conditions required for the deposition process pose significant challenges. Additionally, PVD is limited by the maximum achievable film thickness, which is typically around 10 μm – a limitation that can be addressed through spraying techniques. Among PVD methods, magnetron sputtering has emerged as the preferred process for depositing a variety of industrially significant coatings. This preference is driven by the growing demand for high-quality

* *E-mail: kmzx201@163.com*

functional films across diverse market sectors, where magnetron sputtering has made a substantial impact.

Copper (Cu) is generally used for surface metallization of AlN ceramics. The main methods of AlN surface metallization include the Ti–Ag–Cu active alloy method, activated Mo–Mn method, chemical gold plating method, thick film metallization process [4], sintering method, vacuum coating and brazing method [5], direct Cu coating method [6], and laser cladding [7]. In the process of surface metallization, the selection of an active solder is very important. First, it is necessary to ensure the wetting and welding of the active solder with metal and ceramic parts at the same time. Second, Al and its alloys soften easily at >300°C, which will affect the high-temperature performance of ceramic materials. Therefore, some other alloying elements are generally used to achieve low-temperature welding and high-temperature application [8]. For oxide ceramics, there is accumulation of oxygen ions on the surface of the ceramics. Silicon (Si) is commonly used in electronic components. Titanium (Ti) is currently commonly used as an active agent because the thermal expansion coefficient of AlN ceramics is similar to that of Si, and Ti has a greater affinity for oxygen. The contact angle of liquid pure Cu to AlN is 147° at 1,100°C [9]. The Ag–Cu–Ti active brazing filler is used to braze AlN ceramics with oxygen-free Cu to achieve a gas seal connection between AlN ceramics and oxygen-free Cu. By calculating the free energy of the reaction, the trend of TiN, Ti_2N, Ti_4N_3, and other products can be inferred and compared, consequently predicting the properties of welded joints [3]. This study focuses on the structural metallurgical properties and the formation mechanism of the cladding layer by different process methods with a Ti active agent, providing a theoretical basis for the study of metal cladding on the ceramic surface.

2. Test materials and processes

AlN ceramic sheets with 10 mm × 10 mm × 1 mm dimensions were selected as the substrate material. 300 mesh Cu powder was adopted. In order to increase the moisture of metal on the ceramic surface, Ti powder was added to it. The purity of both was higher than 99.9%. A planetary ball mill was used to evenly mix Cu powder and Ti powder with a mass ratio of 4:1 more than 3 h. The phase composition of the mixture was analyzed by X-ray diffraction (XRD). The detailed testing parameters were as follows: a scanning range of 10°–100°, a step size of 0.01°, and a scanning speed of 15°/min. Cu and Ti did not form intermetallic compounds, which still existed in the form of Cu and Ti, as shown in Figure 1. This shows that the new phase compounds formed by ceramic and Cu substrates were from the metallurgical reaction.

In the laser cladding test, a YAG laser with a power of 700 W was used to prepare the Cu coating on the ceramic surface [10], as shown in Figure 2. First, the AlN ceramic sheet was cleaned with acetone and an ultrasonic cleaner. Ar gas was passed into the Ar gas protective cover for 10 min. Cladding was carried out under the Ar gas

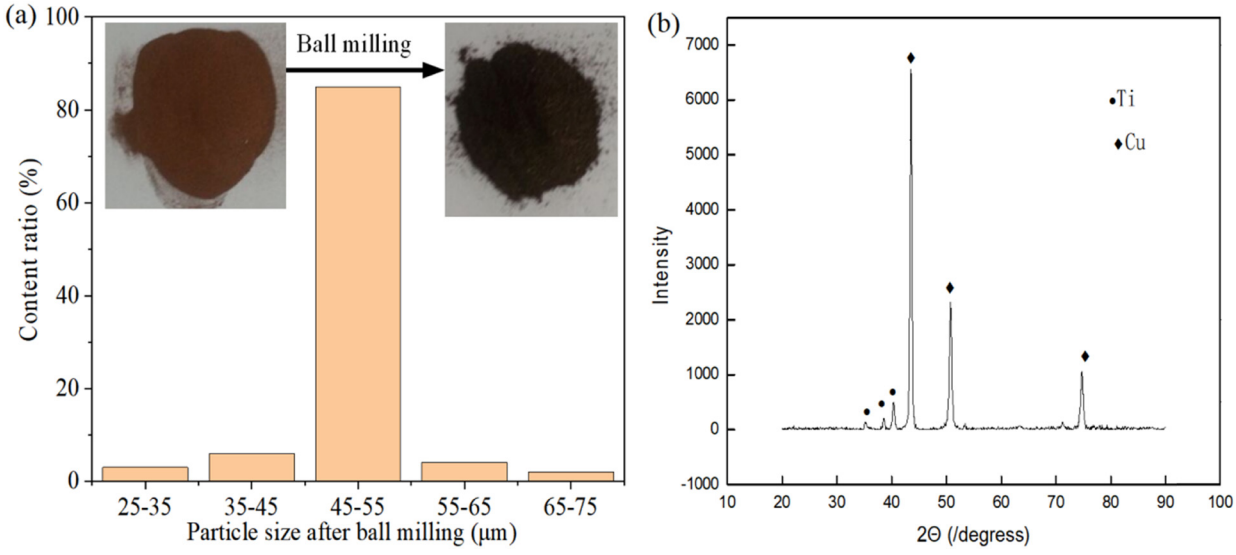

Figure 1. Morphology and phase composition of the clad powder. (a) Morphology of the clad powder before and after ball milling and (b) XRD phase analysis of the ball-milled Cu–Ti powder.

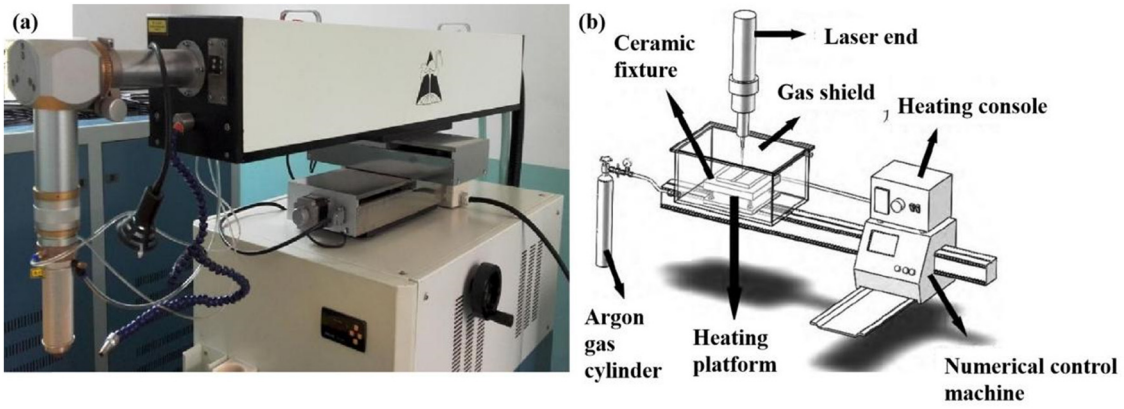

Figure 2. Laser cladding test equipment. Photograph (a) and schematic diagram (b).

protective cover. According to the previous research basis, the main process parameters of laser cladding include the current, pulse width, frequency, and scanning speed. The experimental parameters of the laser are shown in Table 1.

The vacuum brazing furnace [11], as shown in Figure 3, was used to prepare the Cu coating on the ceramic surface. The Cu powder and Cu–Ti powder were uniformly coated on the ceramic surface and heated to a certain temperature in the vacuum brazing furnace to keep it warm, then cooled to 400°C with the furnace, and finally cooled to room temperature.

3. Formability characteristics of the cladding layer

Under the protection of Ar, the Cu substrate clad on the ceramic surface has a shining metallic surface. The Cu and Ti powder clad on the ceramic surface was uniform with excellent macromorphology. The Cu coating was firmly coated on the ceramic surface, as shown in Figure 4. The microstructure of the ceramics combined with Cu coating is shown in Figure 5. Obviously, a shiny transition layer is shown. The thickness of the transition layer is about 3–5 μm. There are no obvious cracks, pores, and other defects between the Cu coating and the ceramic sheet.

According to the microstructure of Cu coating and ceramics, excellent formability is clearly seen. Metallurgical connection is shown between the ceramic surface and the Cu–Ti powder after the laser reaction. The shining transition layer in the figure is the metallurgical reaction area, where the compounds, such as Ti_3Al, TiAl, $TiAl_3$, and metal oxides, are formed. The specific compounds formed by the transition layer need to be analyzed by XRD later to conclude whether the bright ribbon is a new material binding layer after the metallurgical reaction.

4. Metallurgical bonding mechanism of the cladding layer

4.1 Cladding layer by brazing

Using the scanning electron microscopy (SEM) test, the microstructure of the brazed cladding layer was observed, as shown in Figure 6. There is an obvious transition layer at the interface of the ceramic and Cu cladding layer. The content of Ti element was determined to be 60.3% by scanning the marked area. The N element in AlN ceramics penetrates the metal coating, further forming a new compound phase by the metallurgical reaction with Cu and Ti near the transition layer. Line scan analysis of the path is shown in Figure 7, which exhibited consistent test results with the former research [11]. The change in the elemental ratio is marked in the figure. It can be seen that the ratio of Ti increases obviously in the transition layer until it reaches a stable level. The ratio of Ti decreases certainly

Laser parameter	Value
Electric current	200 A
Pulse width	2.0 ms
Laser frequency	4 Hz
Scanning speed	355 mm/min

Table 1. Laser cladding process parameters.

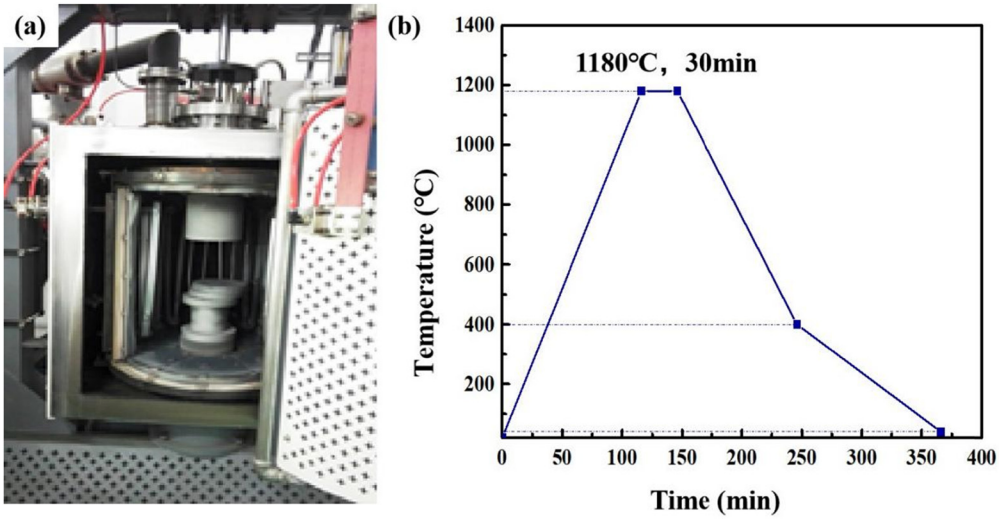

Figure 3. Brazing and cladding test equipment (a) and brazing thermal evolution process (b).

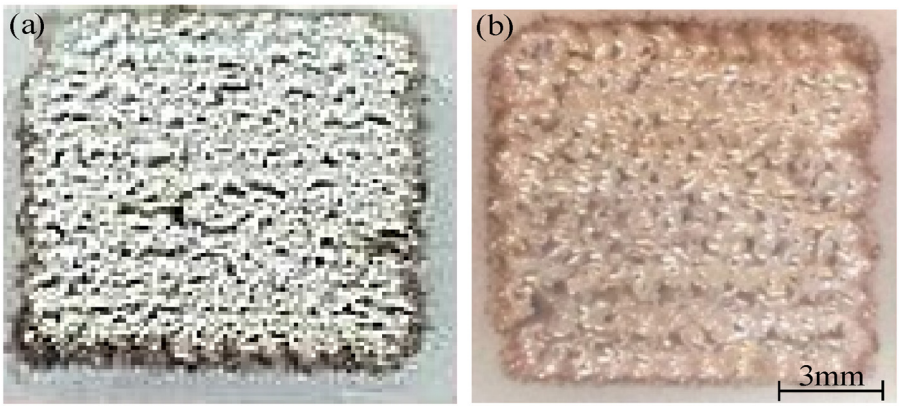

Figure 4. Macromorphology of Cu cladding coated by (a) brazing and (b) laser [12].

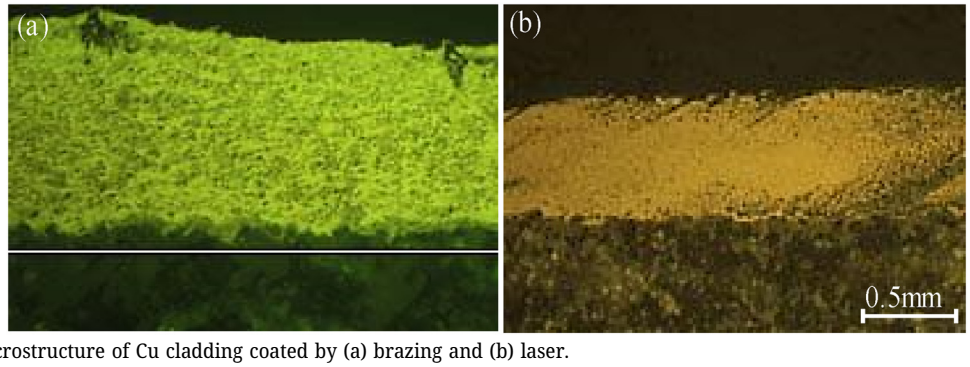

Figure 5. Microstructure of Cu cladding coated by (a) brazing and (b) laser.

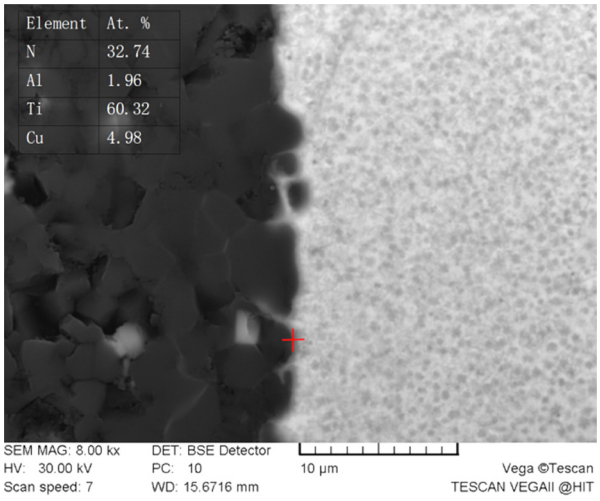

Figure 6. Scanning results of the interface points of brazing between the ceramic and Cu cladding.

with the gradually increasing ratio of Cu. The content of N element increases at the interface between the ceramic sheet and Cu coating, followed by a decrease because a new phase is formed after the reaction with N in AlN and Ti.

The N element in AlN ceramics penetrates the metal coating. The metallurgical reaction occurs with Cu and Ti near the transition layer, and a new compound phase is formed. According to the changes in the elemental content, as shown by the line scan, Ti–Cu binary phase diagram, and Ti–Al binary phase diagram, a schematic diagram of the metallurgical reaction in the transition layer can be made, as shown in Figures 8 and 9, respectively [13]. TiN is synthesized on the left side of the transition layer because the ratio of Ti increases with the N element. Ti_3Al is synthesized in the middle of the transition layer. $TiCu_2$ intermetallic compounds are synthesized on the right side of the transition layer.

4.2 Cladding layer by laser

Under the atmosphere of Ar, XRD phase analysis was performed on the Cu cladding layer of the ceramic surface by

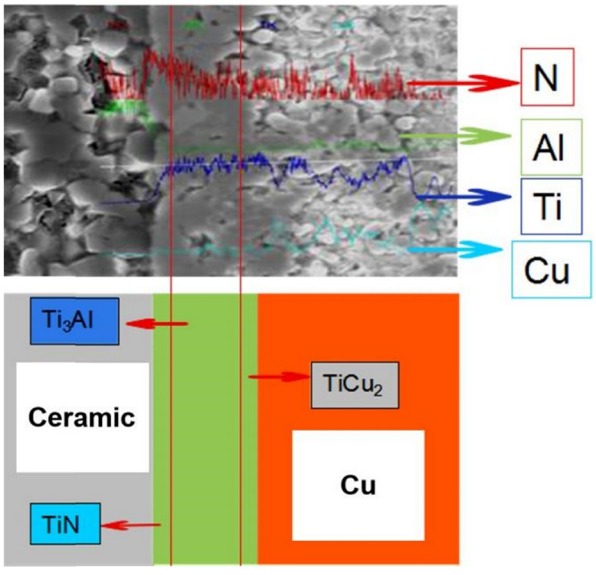

Figure 7. Schematic diagram of the metallurgical reaction in the brazing transition layer.

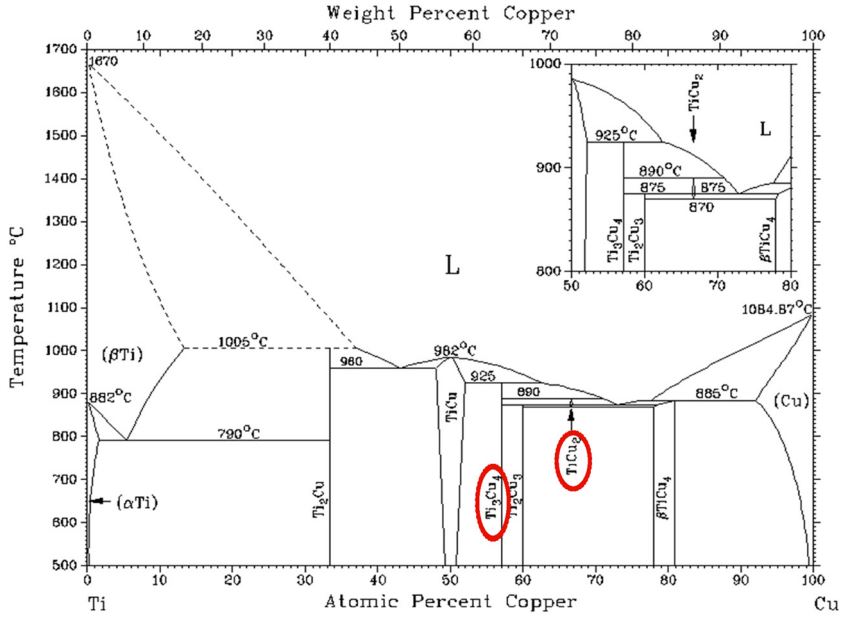

Figure 8. Ti–Cu binary phase diagram [13].

laser melting. The details of testing parameters are as follows: a scanning range of 10°–100°, a step size of 0.01°, and a scanning speed of 15°/min. As shown in Figure 10 [10], TiAl, Ti_3Al, Cu_4Ti_3, and Ti_2N compounds were synthesized during the preparation of the Cu cladding layer on the ceramic surface by laser melting. The scan analysis of the transition layer is shown in Figure 11. The change in the contents of N, Ti, Al, and Cu is shown in Figure 12. AlN ceramics, transition layers between ceramics and metal layers, and metal layers are shown in Figure 12 from left to right. As can be seen from the figure, the content of N element in AlN ceramics is relatively high with 30–40%, and the content of N element near the surface is declining. The content of N element in the metal layers is about 10%. The content of Al in the AlN ceramic is very high, and the content of Al in the transition layer gradually decreases.

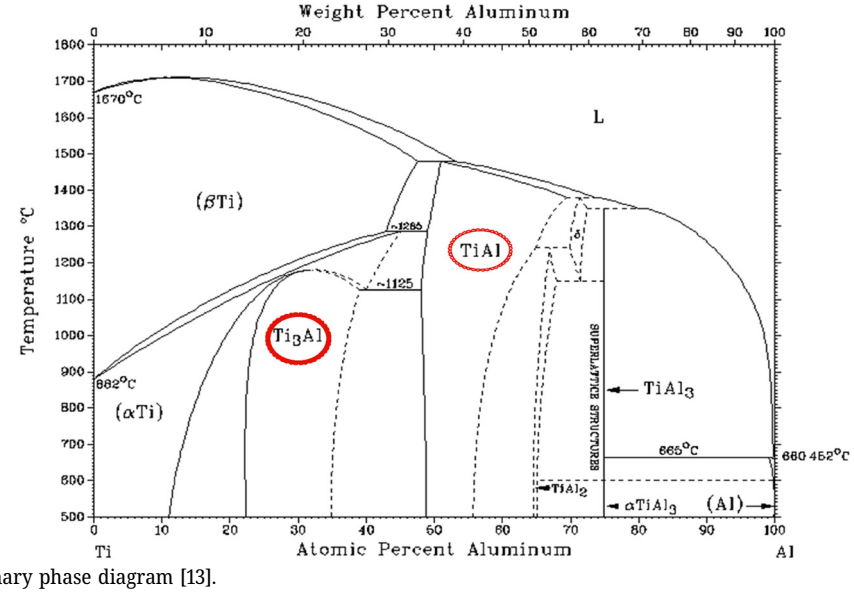

Figure 9. Ti–Al binary phase diagram [13].

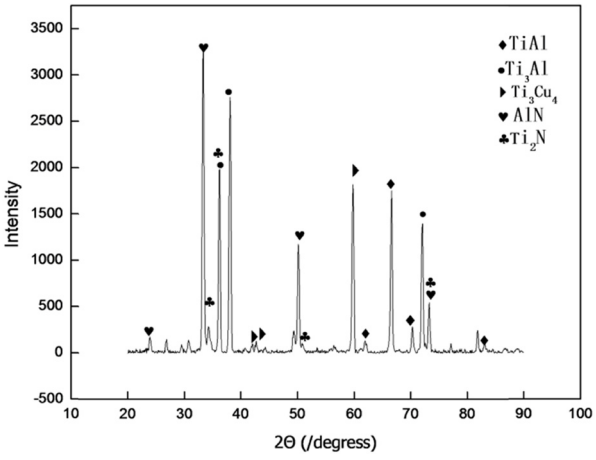

Figure 10. Phase analysis of Cu-coated metal layers on the ceramic surface under the atmosphere of Ar.

The content of Al is extremely small until the metal layer. The content of Ti in the AlN ceramic decreases with almost 0%. The content of Ti in the transition layer increases sharply, and the content of Ti in the metal layers decreases gradually. This fully shows the excellent wettability of Ti, which plays a great role in promoting the reaction layer of ceramics and metal. The content of Cu from the AlN ceramic to the metal layers also increases gradually. The content of Cu in the transition layer shows an increasing trend.

According to the line scan, XRD phase, and the changing content of Cu, Ti, Al, and N, the metallurgical reaction diagram can be made by the laser, which shows Cu-coated metal layers of the transition ceramic surface. As shown in Figure 12, the left side shows the ceramic sheet. The middle is the transitional area with the metallurgical reaction. The right side is the Cu-coated layer area. The Cu content of the left side of the transition layer is very low. Al penetrates the metal layers from AlN ceramics to take part in the metallurgical reaction. The content of Al on the right side of the transition layer is extremely low. The content of Ti remains relatively high over the whole transition layer. There is a platform where the content of N fluctuates within a small range. Therefore, the distribution of compounds in the transition layer can be concluded (Figure 12). The left side of the transition layer is mainly Ti_3Al and TiAl, and the right side of the transition layer is Ti_3Cu_4, while Ti_2N is distributed over the whole transition layer.

In order to gain a clear understanding of the microstructure of the transition layer and the changes in elements near the transition layer, analysis of the transition

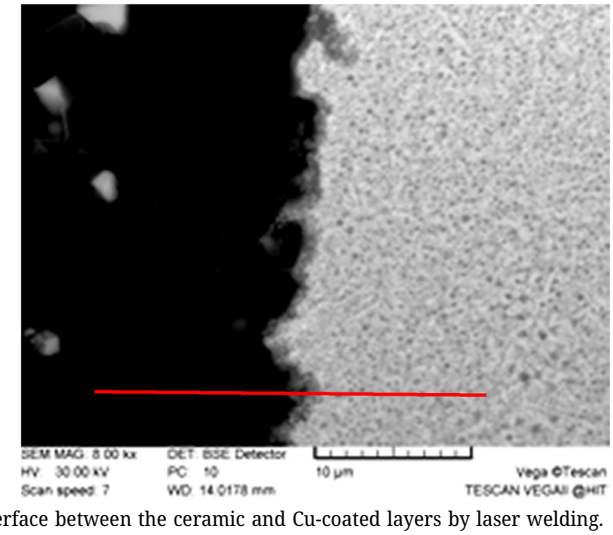

Figure 11. Scanning path of interface between the ceramic and Cu-coated layers by laser welding.

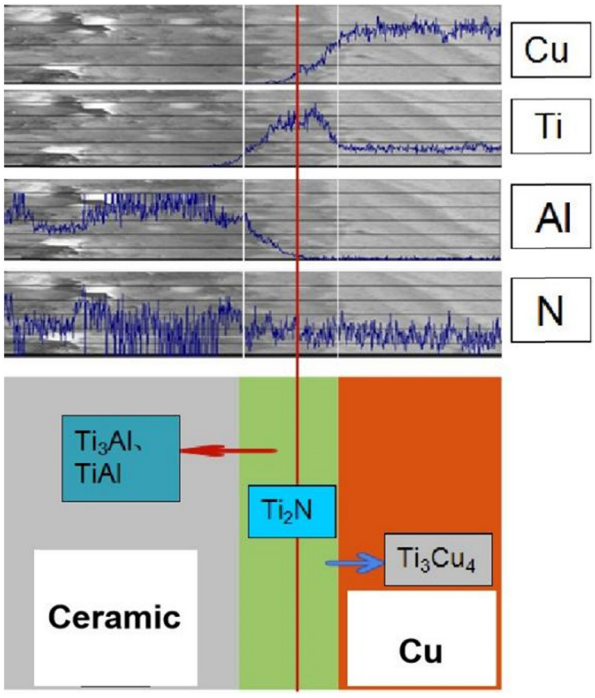

Figure 12. Metallurgical reaction diagram of the transition layer by laser cladding.

layer between the Cu-based metal coating and the ceramic substrate using SEM revealed a clear transition layer between the Cu-based metal coating and the ceramic substrate. Additionally, EDX analysis of the transition layer revealed the presence of Cu [14], and the changes in the content of elements such as Ti, Al, and N. During the laser cladding process, oxygen in air enters the transition layer and combines with the metal, resulting in a characteristic phenomenon of increasing and then decreasing oxygen content near the transition layer.

During the laser cladding process, microarea scanning and phase analyses indicate that a reaction occurred between the Cu-based metal coating and the ceramic substrate, forming a metallurgical bond.

5. Conclusions

(1) By brazing the pure Cu powder and Cu–Ti alloy powder on the ceramic surface, the Cu powder with Ti element is evenly spread on the ceramic surface, and Ti, as an active element, can improve the wettability of the Cu powder on the ceramic surface.

(2) By laser cladding, the Cu substrate reacts with the AlN ceramic at the interface and form a good metallurgical combination. The shining transition layer in the figure is the metallurgical reaction area, where compounds, such as Ti_3Al, TiAl, $TiAl_3$, and metal oxides, are formed. However, by brazing cladding, the interfacial metallurgical reaction process is more full, the thickness of the transition layer is larger, and the integrity of the ceramic sheet is higher under an inert gas environment.

(3) The active element Ti is distributed mainly in the transition layer, and it reacts with Cu in the ceramic matrix and the metal layers, realizing the metallurgical reactions at the same time, producing TiO_2, Ti_3Al, Cu_4Ti_3, Al_2TiO_5, etc., thus forming a metallurgical combination between the ceramic and the metal coating.

Acknowledgments

The results of this paper depend on the data collected by the test center, and we thank the test center of Sun Yat sen University for providing a high standard of experimental data for this study.

Funding information

This work was financially supported by Special Project for Investigation of Science and Technology Basic Resources

by the Ministry of Science and Technology (NO. 2022FY101302).

Author contributions

Song Wang and Xin Zhang: Conceptualization, Methodology. Hao Lu and Fengyuan Shu: Data curation, Writing – original draft. Fengyuan Shu and Xin Zhang: Visualization, Investigation. Xin Zhang: Supervision. Xin Zhang and Guibian Li: Writing – review & editing. Song Wang, Hao Lu and Guibian Li: Methodology, Data curation.

Conflict of interest statement

The authors declare that they have no known competing financial interests or personal relationships that could have appeared to influence the work reported in this paper.

References

[1] Rubio-Marcos, F., Romero, J.J., Navarro-Rojero, M.G., Fernandez, J.F., Effect of ZnO on the structure, microstructure and electrical properties of KNN-modified piezoceramics, J. Eur. Ceram. Soc., 2009, 29(14): 3045–3052

[2] Comas, T.F., Diao, C., Ding, J., Williams, S., Zhao, Y., A passive imaging system for geometry measurement for the plasma arc welding process, IEEE Trans. Ind. Electron., 2017, 64(9): 7201–7209

[3] Zhao, Y.X., Wang, M.R., Cao, J., Song, X.G., Tang, D.Y., Feng, J.C., Brazing TC_4 alloy to Si_3N_4 ceramic using nano-Si_3N_4 reinforced AgCu composite filler, Mater. Des., 2015, 76: 40–46

[4] Zhou, Y., Sun, Z., Electronic structure and bonding properties of layered machinable Ti_2AlC and Ti_2AlN ceramics, Phys. Rev. B., 2000, 61(19): 12570

[5] Shu, F., Numerical simulation and experimental study on rapid preparation of copper coating on AlN ceramic surface [D]. Harbin Institute of Technology, Harbin, 2010 (In Chinese)

[6] Liu, D., Chen, N., Song, Y., Song, X., Sun, J., Tan, C., et al., Mechanical and heat transfer properties of AlN/Cu joints based on nanosecond laser-induced metallization, J. Eur. Ceram. Soc., 2023, 43(5): 1897–1903

[7] Schreck, S., Rohde, M., Local modification of ceramic surfaces by a laser induced cladding process [C]. Conference on laser-based micro- and nanopackaging and assembly III; 20090128-29; San Jose, CA (US). Forschungszentrum Karlsruhe GmbH, Institute for Materials Research I, Hermann-von-Helmholtz-Platz 1, 76344 Eggenstein, Germany; Forschungszentrum Karlsruhe GmbH, Institute for Materials Research I, Hermann-von-Helmholtz-Platz 1, 76344 Eggenstein, Germany, 2009

[8] Lei, J., Shi, C., Zhou, S., Gu, Z., Zhang, L.C., Enhanced corrosion and wear resistance properties of carbon fiber reinforced Ni-based composite coating by laser cladding, Surf. Coat. Technol., 2018, 334: 274–285

[9] Yang, Z.W., Zhang, L.X., Xue, Q., He, P., Feng, J.C., Interfacial microstructure and mechanical property of SiO_2-BN ceramics and Invar joint brazed with Ag-Cu-Ti active filler metal, Mater. Sci. Eng. A., 2012, 534: 309–313

[10] Wang, J.X., Chuang, K.H., Wu, Y.C., Mechanical performances of AlN/Al metallized ceramic substrates fabricated by transient liquid phase bonding and pre-oxidation treatment, Ceram. Int., 2022, 48(12): 16619–16629

[11] Zhao, J., Wang, X., Shu, F., Jiang, S., Ma, P., Zhao, Y., et al., Research on microstructure of copper coatings on AlN ceramic surface by laser cladding and brazing, Mater. Res. Express, 2020, 7(7): 075104

[12] Xiong, L.D., Wang, C.J., Wu, W., Xu, L.J., Wang, C.M., Deng, H., et al., The surface softening mechanism of AlN ceramic by laser treatment, Surf. Interfaces, 2024, 46: 104023

[13] Singleton, M.F., Nash, P., Binary alloy phase diagrams, 2nd ed. (Ed. T.B. Massalski), ASM International, Tennessee, USA, 1990

[14] Zhang, M.H., Zhao, C., Bai, J.M., Hu, Z.Y., Cai, J.W., Zhang, Z.R., et al., Enhancing thermal conductivity of AlN ceramics via vat photopolymerization through refractive index coupling and oxygen fixation, Addit. Manuf., 2024, 95(5): 104522